Identifying Unknown Materials with X-Rays by Testing Moseley's Law and Bragg's Law

Hyun Wallace Anderson

The Ohio State University, Physics Department, Columbus, Ohio, 43210

In this experiment, characteristic x-rays from various known and unknown elements will be measured in order to test Moseley's law and Bragg's law. Moseley's law will be tested by determining the frequency of characteristic x-rays of known metals and creating a Moseley plot; fitting the data to judge the proportionality. Bragg's law is tested by identifying the angle at which peak x-ray diffraction occurs in crystals to ascertain the distance between their atomic lattice planes. In conducting these experiments, we find that Moseley's law accurately relates K and L-shell x-ray emissions to their atomic number, and in testing Bragg's law, we find that x-ray diffraction indeed occurs and allows us to find the distance between crystal lattice planes.

Introduction

In 1913, Niels Bohr and Ernest Rutherford postulated a model of the atom in which a positive nucleus is orbited by electrons confined to atomic shells by electrostatic attraction: for an illustration see **S.I. 2**. Using Bohr's model as its foundation, Henry Mosley derived a law which states that the square root of the frequency of a characteristic x-ray emitted by an atom is proportional to its atomic number[1], as detailed in equation (1). Before Moseley's law, the atomic number of an atom did not correspond to any measurable quantity. Concurrently, Laurence and William Henry Bragg discovered that crystalline solids defracted characteristic x-rays when hit from an incident angle which is unique to the crystal[2]. Bragg's law occurs under specific x-ray wavelengths that are whole number multiples of the distance between crystal lattice planes, which is illustrated in **Fig. 2** and equation (2).

The purpose of this experiment is to test Moseley's law and Bragg's law using known materials in order to identify unknown materials. We will test Moseley's law by plotting the square-root of the frequency of characteristic x-rays for various elements as a function of their atomic number, judging their proportionality by fitting them to equation (1). For this, the energy of K and L-shell x-ray emissions for various metal samples are identified using a Si-PIN Detector and their frequency is calculated using Bohr's solution for hydrogen: equation (1.1). We will test Bragg's law by calculating the distance between crystal lattice planes and comparing the results with accepted values. For this, x-ray intensity over a range of angles is measured with a Geiger-counter to find the angle of peak diffraction for various crystals. Using the wavelength of the x-ray and the angle of incidence, we will calculate lattice distance with equation (2). Through this experiment we find that Moseley's law accurately describes our results for K and L-shell x-ray emissions; and the unknown metal is determined to be monel, a nickel-copper alloy. We also find that x-ray diffraction indeed occurs under the conditions outlined by Bragg's law, allowing us to calculate the lattice distance of crystals; and the unknown crystal is determined to be potassium-bromide (KBr).

Theory

Before approaching the experiment, it is useful to understand the process of *X-Ray Fluorescence* (or *XRF*), which is used to identify types and amounts of elements present in a material. In an x-ray tube, a beam of electrons is accelerated through high electrical potential between a heated cathode and a copper anode target, as seen in **S.I. 1**. These electrons strongly decelerate when they come into contact with the electromagnetic forces in the cathode, producing continuous x-rays known as *Bremsstrahlung* (or breaking radiation). Once the bombarding electrons force an electron within the target material to be ejected from its shell, its vacancy is filled by a donor electron dropping from a higher orbital. The donor electron loses energy in this transition

and a photon of energy ΔE is released equal to the difference in potential between orbitals as detailed in equation (1.1): this is a *characteristic x-ray* of the material. On a plot of intensity as a function of energy, Bremsstrahlung is characterized by a continuous spectrum, while the characteristic x-rays are sharp peaks of intensity as seen in **Fig. 5**.

Moseley's Law states[1]: the square-root of the frequency of an x-ray emitted by an atom is proportional to its atomic number, as seen in equation (1). Moseley uses Bohr's solution for hydrogen, which relates energy to frequency for an electron transition, as seen in equation (1.1). For a derivation of Moseley's Law, see **Appx. A**. For details on x-ray notation see **S.I. 2**.

$$\sqrt{v} = A(Z - b) \propto Z \qquad \textbf{(1)} \qquad\qquad \Delta E = hv = E_i - E_f \qquad \textbf{(1.1)}$$

Where v is the frequency of the observed x-ray emission line, Z is the number of protons in the atom, h is Planck's constant in eV·s, and A and b are constants that depend on the x-ray emission type (K or L, in x-ray notation) as seen in equations (1.1) and (1.2):

$$A = \left(\frac{1}{1^2} - \frac{1}{2^2}\right) R_y,\ b = 1\ for\ K_\alpha \qquad \textbf{(1.2)} \qquad\qquad A = \left(\frac{1}{2^2} - \frac{1}{3^2}\right) R_y,\ b = 7.4\ for\ L_\alpha \qquad \textbf{(1.3)}$$

Bragg's Law states[2]: if an x-ray reflects off a crystal at an angle equal to the angle of incidence and has a wavelength that is a whole number multiple of the distance between the crystal's atomic lattice planes, a constructive interference will occur. Therefore, by knowing the wavelength of an x-ray and identifying the peak angle of diffraction for a crystal, one can characterize a crystal's structure. In this experiment, the characteristic x-ray of the copper anode is used as the incident x-ray. Bragg's law (2), is derived as follows using the lattice geometry as seen in **Fig. 2**:

$$n\lambda = \overline{AB} + \overline{BC} \qquad \textbf{(2.1)}$$

$$\overline{AB} = \overline{BC} = 2dsin(\theta) \qquad \textbf{(2.2)}$$

$$n\lambda = 2dsin(\theta) \qquad \textbf{(2)}$$

Where: n is the diffraction order, λ is the wavelength of the x-ray, d is the distance between lattice planes, and θ is the incident angle.

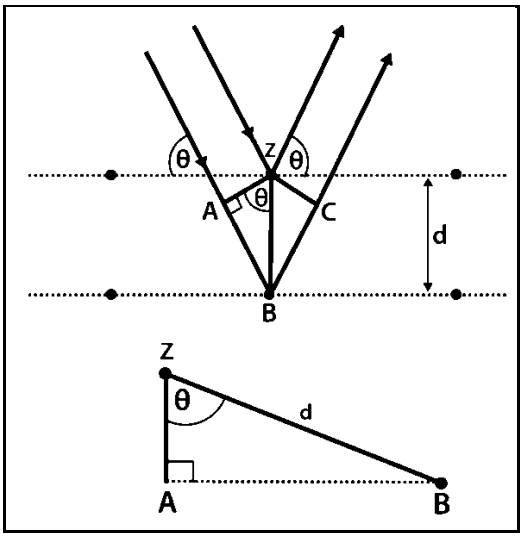

Figure 2: Geometry of Crystal Lattice Planes in Derivation of Bragg's Law. *(dotted-lines denote lattice planes, dots are atoms, and arrows are x-rays).*

Experimental Methods

The apparatus for which we will be conducting our experiments is a TEL-X-Ometer x-ray machine produced by TEL-Atomic, as seen in **Fig. 3**. When testing Moseley's law, a Si-PIN detector is placed in the carriage arm which measures x-ray intensity as a function energy bins. We create a calibration curve for the Si-PIN detector so we may precisely relate bin width to energy (keV); the details of this process are in **Appx. B**. Once the calibration is made, a metal sample is placed on the rotating platform of the x-ray machine at a fixed 45° angle θ relative to the x-ray tube and the detector in the carriage arm is fixed in position at 90° 2θ. The x-ray machine is turned on and the sample is bombarded with x-rays for several

minutes while a computer records the detector's output as a function of energy. This process is repeated for each sample; for a table of all elements tested, see **Appx. C**. Once the K or L-shell x-ray emissions for each element are found, a Moseley plot of the square root of the frequency of these x-rays as a function of atomic number is fit to equation (1). This process also allows us to calculate the wavelength of copper x-rays using equation (1.1) so that we may test Bragg's law; seen in **Appx. D**.

When testing Bragg's law, we are interested in x-ray intensity as a function of angle, so the detector is switched to a Geiger-counter and the crystal platform and carriage arm are allowed to rotate by the use of motors. A series of lead collimators are placed in front of the Geiger-counter for focus. Each crystal sample is placed on the rotating platform at the center of the x-ray machine and a wide range of angles are scanned over a short period of time in order to identify the most intense peaks. This is followed by a finer scan of the peaks, spending 15 seconds 0.1° 2θ increment. For a table of all crystals tested as well as their plots, see **Appx. E**. The angle θ at which the diffraction peaks are located is used to calculate the distance d between lattice planes using equation (2) and the difference between the known distances[4] and the calculated values will determine the accuracy of Bragg's law.

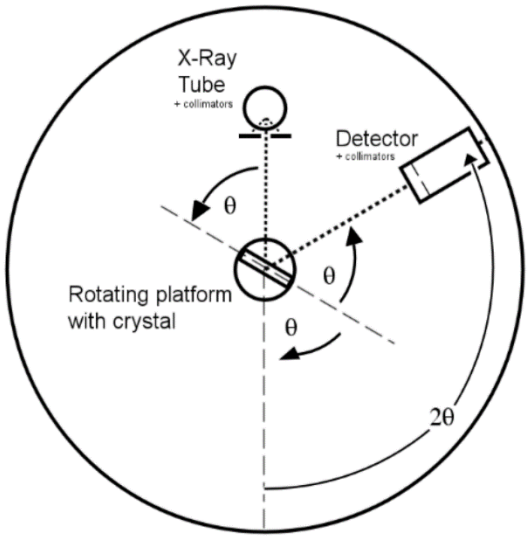

***Figure 3: TEL-Atomic X-Ray Machine**. The machine consists of three main components, an x-ray tube, a rotating platform for holding target materials, and a rotating carriage arm that holds detector instruments. The rotating platform turns at an angle θ perpendicular to the x-ray tube, and the carriage arm (detector) turns at a 2θ orientation relative to the incident x-rays. All experimentation is done with the x-ray tube voltage set to 30keV and with a current of approximately 60μA.*

Results

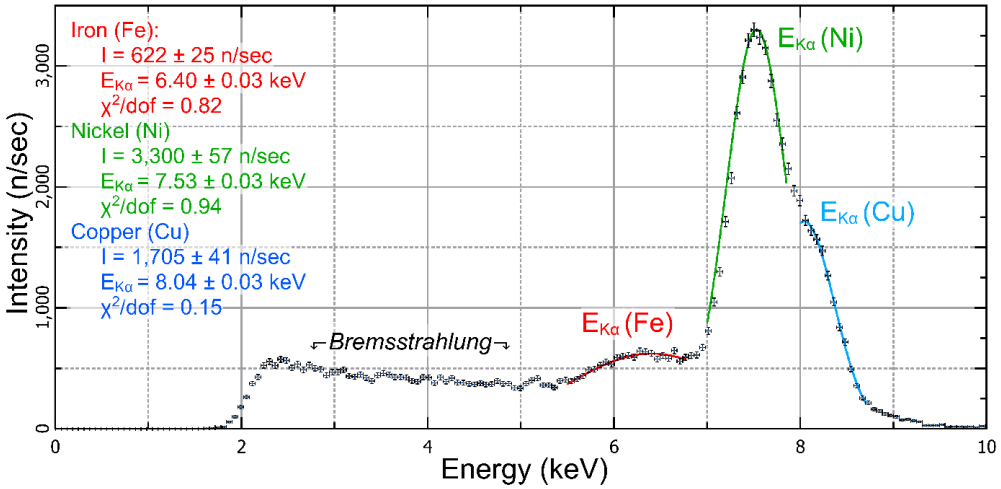

***Figure 4: Characteristic X-Rays of Unknown Metal.** Intensity plotted as a function of energy. Bremsstrahlung radiation can be seen from approximately 2 – 5keV. Three $K_{\alpha 1}$ emissions are fit to gaussians, with the centroid of Fe (red) located at 6.40keV, Ni (green) at 7.53keV, and Cu (blue) at 8.04keV. Determined to be nickel-copper alloy "monel". Error in intensity is the square root of n, per the Poisson distribution and error in energy is half the bin to energy conversion factor.*

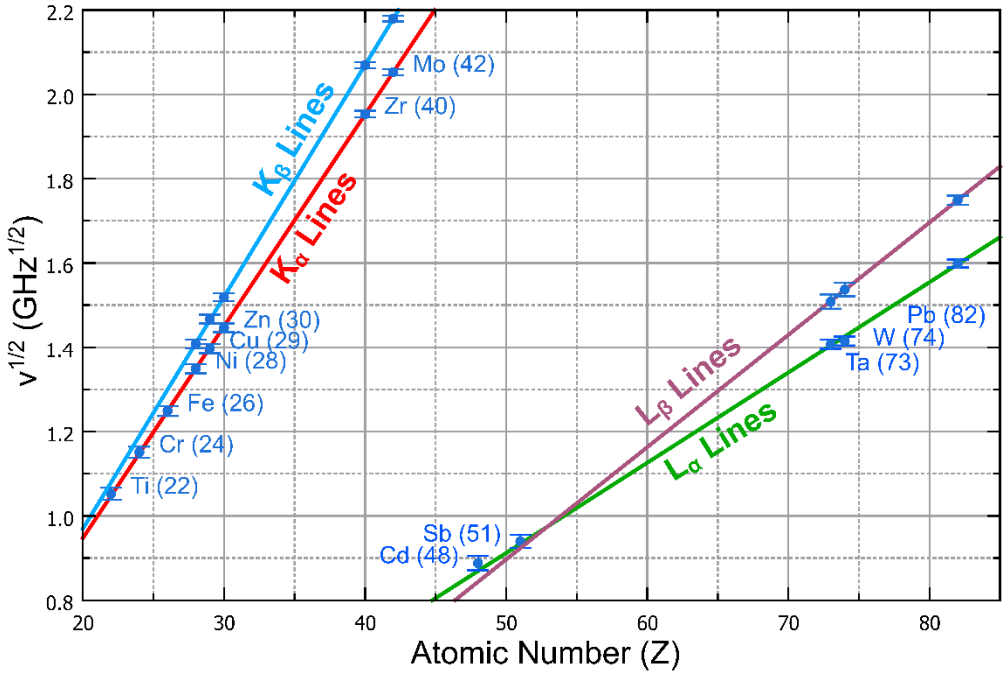

Figure 5: Moseley Plot. *The square root of frequency v as a function of atomic number Z for 12 unique elements, between three linear fits for $K_{\alpha 1}$ (red), $K_{\beta 1}$ (green), $L_{\alpha 1}$ (blue), and $L_{\beta 1}$ (purple) emission lines. Each element is shown next to its respective data point sequentially from bottom to top, with its atomic number in parenthesis. Error in frequency propagated from bin-width error.*

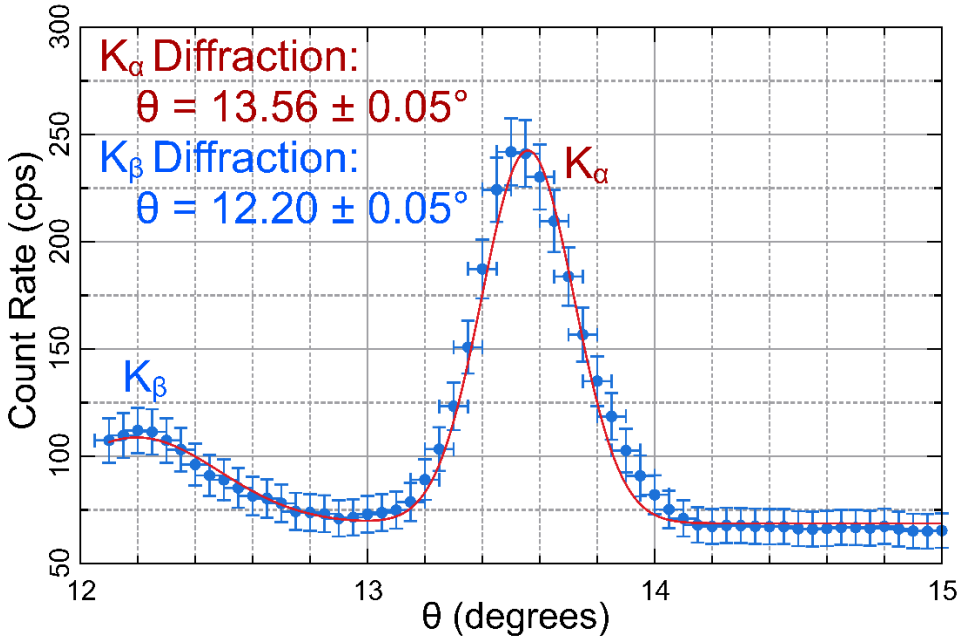

Figure 6: Bragg Diffraction for Unknown Element. *Count rate as a function of incident angle θ (converted from 2θ of detector arm) for unknown crystal. Diffraction angles found for $K_{\alpha 1}$ (red): $\theta = 13.56^{\circ}$; $K_{\beta 1}$ (blue): $\theta = 12.20^{\circ}$. Error in counts is the square root of n, per the Poisson distribution, error in θ from carriage arm lag relative to intended angle.*

Discussion and Conclusions

Moseley's law appears to accurately relate K and L-shell x-rays to their atomic number as seen in **Fig. 5**, and each emission line appears to fit equation (1), as seen in a table of reduced χ^2 tests in **Appx. C**. Though the fitted values for A and b are close to theory they were greatly overfitted suggesting that the estimated error is too large. It should be noted that Moseley's law is unlikely to work for higher-order emissions. This is because Moseley's law forms its basis from the Bohr model of the atom which itself is a first-order approximation of the hydrogen atom. Though useful in approximations such as this, the Bohr model is considered obsolete and has since been replaced by the *Electron Cloud Model*.

We estimate the identity of the unknown metal is a nickel-copper alloy such as monel. The sample contains three identifiable characteristic x-ray peaks as seen in **Fig. 4**, which are estimated to be iron (0.06% difference from purported), nickel (0.70%), and copper (0.10%). Assuming the measured x-ray intensity equates to relative content, it is likely not a cupronickel alloy (CuNi) due to the low percentage of copper; cupronickel must have a minimum copper content of 60% whereas in the sample it is 51.57% of the intensity of nickel. Monel is a better fit as it has a nickel content of between 52 – 67%. Both candidate alloys contain a small amount of iron which is of a normal proportion in our sample.

Our test of Bragg's law yielded calculations of lattice distance which are quite close to their purported values[4], as seen in **Appx. E**. We estimate that the identity of the unknown crystal is potassium-bromide (KBr). The calculated lattice distance is 3.284±0.027Å for the $K_{\alpha 1}$ reflection and 3.289±0.027Å for the $K_{\beta 1}$ reflection with a percent difference of 0.42% and 0.27% respectively from the purported distance of 3.298. Admittedly, our calculated distance is closer to that of rubidium-chloride (RbCl) with a distance of 3.291Å, although its natural state is a fine crystalline powder, which is unlike the large solid crystal we sampled which is visually similar to KBr. Both candidate crystals are within the margin of error for our calculations.

The main source of error in measuring characteristic x-rays comes from the detector. Since energy must be quantized into discrete bins an error of half a bin width, or 0.03keV is estimated, as seen in **Appx. B**. Assuming an error of one standard deviation of an energy centroid width yields a similar result. Bin width error is of a magnitude which dominates propagation. This is the error used when finding the square root of frequency in the Moseley plot and the wavelength of copper for crystal diffraction, as seen in **Appx. D**. It should be noted that elements that were sampled as part of an alloy or compound yielded a higher percent error in comparison to samples of individual elements. One possible explanation is that in having multiple elements there are more emissions coinciding with the energies of other x-rays, obfuscating their position. For crystal diffraction, the main source of error is found from the motor of the carriage arm lagging behind the angle of crystal mount, though it was a consistent $\pm 0.05^{\circ}$ between all fine measurements. The experiment could be improved by using a motor which is more accurate. Finally, both the detector and Geiger-counter measure x-ray intensity as a count of discrete random events: a Poisson distribution. Therefore, the error in count rate is quite large relative to sample size and can lead to overfitting of the data. For example, the diffraction angles measured were overfitted as seen in **Appx. E**, and since the difference in lattice distance between crystals can be less than 0.01Å, a small change in measured angle makes a large difference. This is why the lattice distances for both RbCl and KBr fall within the error of our calculations.

In conclusion, both Moseley's law and Bragg's law worked as expected under the conditions of our experiment. It appears that the square root of the frequency of K and L-shell emissions are indeed proportional to their element's atomic number, and x-ray diffraction indeed occurs under the conditions stated by Bragg's law. We were able to utilize both laws in identifying unknown materials, finding that the unknown metal is most likely the nickel-copper alloy monel, and the crystal is likely potassium-bromide (KBr).

Citations and References

1. H.G.J. Moseley M.A. XCIII. The High-frequency Spectra of the Elements. The London, Edinburgh, and Dublin Philosophical Magazine and Journal of Science, (1913).

2. Bragg, William Henry and Bragg, William Lawrence. The Reflection of X-Rays by Crystals, Nature 91, 477 (1913).

3. Thompson, A. C. X-Ray Data Booklet (2nd ed.). Lawrence Berkeley National Laboratory, University of California, (2009).

4. Kittle. Table 1. Table of crystal properties. Introduction to Solid State Physics (7th ed.), (1996).

Appendix A: Derivation of Moseley's Law

Moseley's Law was derived empirically by line fitting the square roots of the x-ray frequencies plotted by atomic number, though it can be explained in terms of Bohr's solution of hydrogen:

$$\Delta E = hv = E_i - E_f = \frac{m_e q_e^2 q_Z^2}{8\varepsilon_0^2 h^2}\left(\frac{1}{n_f^2} - \frac{1}{n_i^2}\right) \qquad \textbf{(A1)}$$

Where: h is Planck's constant in eV·s,
v, is the frequency of the characteristic x-ray,
E_i and E_f are the initial and final energies of the electron that transitions into the vacancy, respectively,
ε_0 is the permittivity of free space,
m_e is the mass of an electron,
q_e is the charge of an electron,
q_Z is the effective charge of the nucleus, also equal to $q_e(Z-b)$,
n_f and n_i are the quantum numbers of the final and initial energy level, respectively.

To begin, we simplify equation (A1) and solve for frequency *v*:

$$v = \frac{m_e q_e^4 (Z-b)^2}{8\varepsilon_0^2 h^3}\left(\frac{1}{n_f^2} - \frac{1}{n_i^2}\right) \qquad \textbf{(A1.1)}$$

Using the definition of the Rydberg constant (A1.2) to define constant *A* (A1.3):

$$R_y = \frac{m_e q_e^4}{8\varepsilon_0^2 h^2} \approx 13.6eV \qquad \textbf{(A1.2)} \qquad A^2 \equiv \left(\frac{1}{n_f^2} - \frac{1}{n_i^2}\right)R_y \qquad \textbf{(A1.3)}$$

Simplifying equation (A1) in terms of (A1.1) and (A1.2):

$$v = A^2(Z-b)^2 \qquad \textbf{(A1.4)}$$

Solving for the square root of frequency *v*:

$$\sqrt{v} = A(Z-b) \qquad \textbf{(1)}$$

$$A = \left(\frac{1}{1^2} - \frac{1}{2^2}\right)R_y,\ b = 1\ for\ K_\alpha \qquad \textbf{(1.2)} \qquad A = \left(\frac{1}{2^2} - \frac{1}{3^2}\right)R_y,\ b = 7.4\ for\ L_\alpha \qquad \textbf{(1.3)}$$

Appendix B: Calibration Curve for Si-PIN Detector & Error

The Si-PIN detector we use to measure intensity quantizes x-ray energy into 512 bins corresponding to a range of approximately 30keV. To determine the precise resolution of each bin, a few samples of known metals are placed on the rotating platform of the x-ray machine at a fixed 45° angle θ relative to the x-ray tube (carriage arm holding the detector at 90° 2θ) and are bombarded with x-rays for several minutes while a computer records the detector's output. Then, the centroid bins of each element's emission lines are plotted against their accepted energies[3]. The linear fit of the plot is used as the calibration curve, as seen in **Fig. B1**.

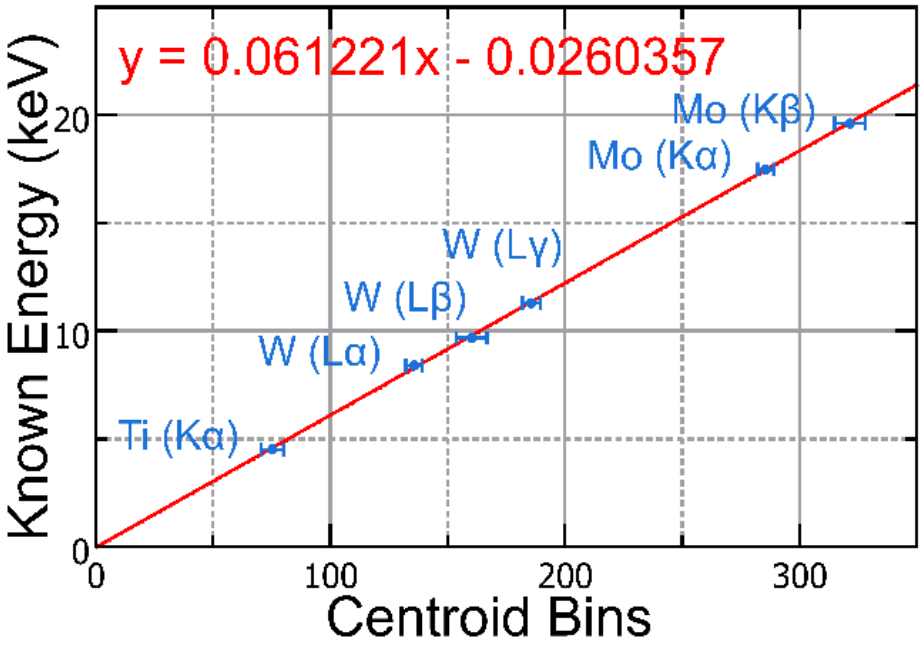

Figure B1: Detector Calibration Plot. *The known energy (keV) of three elements plotted as a function of energy bins (centroid of their characteristic intensity peaks). The three elements in order from left to right are Titanium (Ti), Tungsten (W), and Molybdenum (Mo). The slope from the linear fit acts the correction factor which allows us to relate bins to energy (keV).*

Therefore, the calibration curve is as follows:

$$Energy(bins) = 0.061221 * bins - 0.0260357\ (keV) \qquad \textbf{(B1)}$$

Error in energy is therefore half a bin-width due to quantization of energy:

$$\sigma_E \cong \frac{0.06}{2} = 0.03keV \qquad \textbf{(B2)}$$

Appendix C: Metals Tested for Moseley's Law

Metal	Protons (Z)	Emission Type	Exp. Energy (± 0.03 keV)	Known Energy (keV) [3]	Percent Error (%)	χ^2/dof
Titanium (Ti)	22	$K_{\alpha 1}$	4.59	4.511	1.75	1.95
Iron (Fe)	26	$K_{\alpha 1}$	6.41	6.404	0.09	1.68
Nickel (Ni)	28	$K_{\alpha 1}$	7.53	7.478	0.70	1.42
		$K_{\beta 1}$	8.20	8.265	0.79	1.05
Copper (Cu)	29	$K_{\alpha 1}$	8.07	8.048	0.27	1.17
		$K_{\beta 1}$	8.90	8.905	0.06	1.36
Zirconium (Zr)	40	$K_{\alpha 1}$	15.78	15.775	0.03	1.42
		$K_{\beta 1}$	17.71	17.667	0.24	1.27
Molybdenum (Mo)	42	$K_{\alpha 1}$	17.47	17.479	0.05	1.86
		$K_{\beta 1}$	19.61	19.607	0.02	3.65
Antimony (Sb)	51	$L_{\alpha 1}$	3.65	3.605	1.25	1.94
Tantalum (Ta)	73	$L_{\alpha 1}$	8.15	8.146	0.05	1.27
		$L_{\beta 1}$	9.41	9.343	0.72	1.10
Tungsten (W)	74	$L_{\alpha 1}$	8.29	8.398	1.29	0.63
		$L_{\beta 1}$	9.77	9.672	1.01	0.81
		$L_{\gamma 1}$	11.35	11.285	0.58	1.25
Lead (Pb)	82	$L_{\alpha 1}$	10.57	10.551	0.18	1.43
		$L_{\beta 1}$	12.65	12.614	0.29	1.42
Steel (Cr & Fe)	24 (Cr)	$K_{\alpha 1}$	5.48	5.415	1.20	1.38
	26 (Fe)	$K_{\alpha 1}$	6.42	6.404	0.25	0.55
Brass (Cu & Zn)	29 (Cu)	$K_{\alpha 1}$	8.08	8.048	0.40	1.32
	30 (Zn)	$K_{\alpha 1}$	8.57	8.639	0.80	1.81
Cadmium Paint (Cd & Zn)	48 (Cd)	$L_{\alpha 1}$	3.26	3.134	4.02	0.63
	30 (Zn)	$K_{\alpha 1}$	8.66	8.639	0.24	1.28
		$K_{\beta 1}$	9.54	9.572	0.33	0.32
Unknown	26 (Fe)	$K_{\alpha 1}$	6.40	6.404	0.06	0.82
	28 (Ni)	$K_{\alpha 1}$	7.53	7.478	0.70	0.94
	29 (Cu)	$K_{\alpha 1}$	8.04	8.048	0.10	0.15

Table C1: Sample Metals for Testing Moseley's Law*: In total, 12 unique elements were tested and identified. Exp. Energy is the centroid (μ) of a gaussian fit for an element's characteristic x-rays. Error in energy is half the bin conversion to energy as seen in Appx. B. All the characteristic x-rays of each element can be seen in a Moseley plot in Fig. 5. The unknown element is determined to be a nickel-copper alloy; most likely monel.*

Shell Type	*A* Fit	*A Theory*	*b* Fit	*b* Theory	χ^2/dof
$K_{\alpha 1}$	0.683	0.75	1.138	1	0.06
$K_{\beta 1}$	0.748	*Empirical*	2.370	*Empirical*	0.03
$L_{\alpha 1}$	0.146	0.1388	7.391	7.4	0.83
$L_{\beta 1}$	0.181	*Empirical*	16.33	*Empirical*	0.01

Table C2: Moseley Plot Fitting Results. *Each emission type is fitted to equation (1): A(Z-1). Values for A and b should resemble their definitions as seen in equations (1.1) and (1.2). Values for $K_{\beta 1}$ and $L_{\beta 1}$ are not reported by Moseley and must be found empirically.*

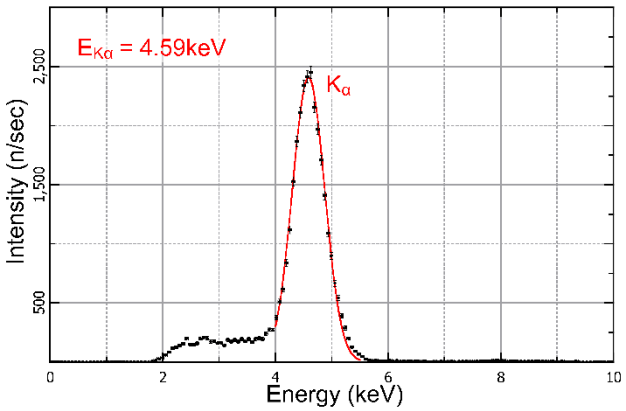

Figure C1: Characteristic X-Ray for Titanium (Ti)

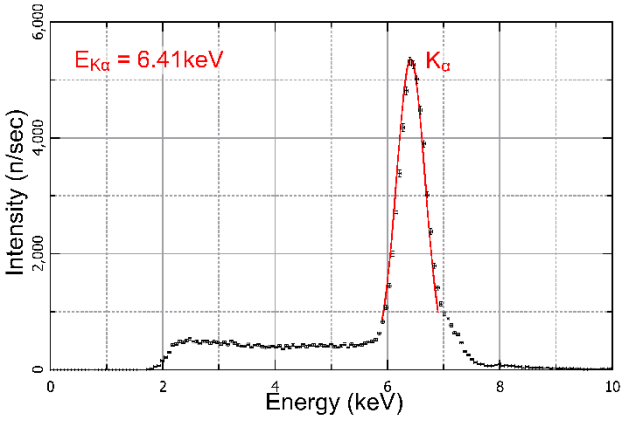

Figure C2: Characteristic X-Ray for Iron (Fe)

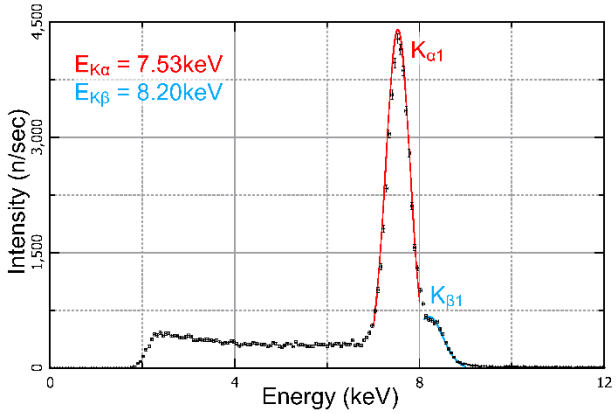

Figure C3: Characteristic X-Ray for Nickel (Ni)

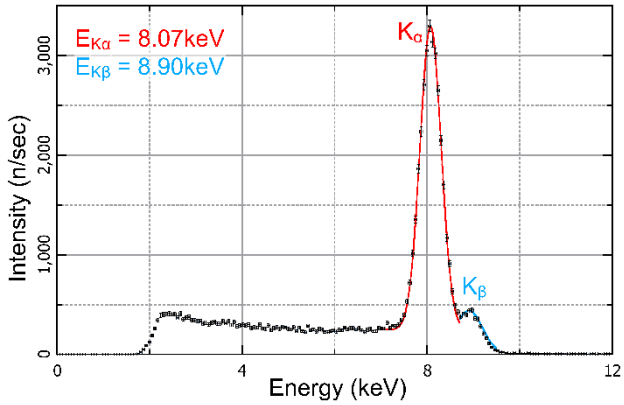

Figure C4: Characteristic X-Ray for Copper (Cu)

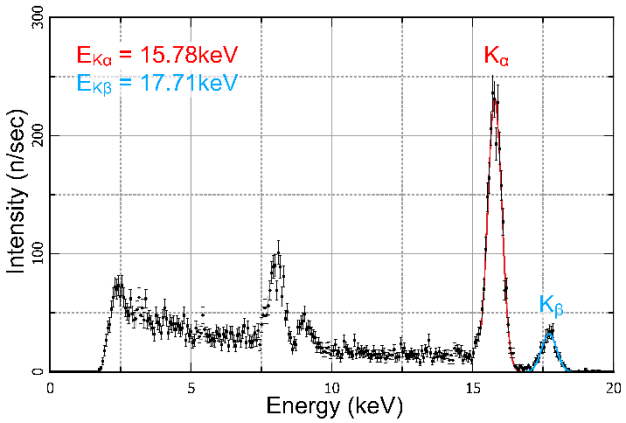

Figure C5: Characteristic X-Ray for Zirconium (Zr)

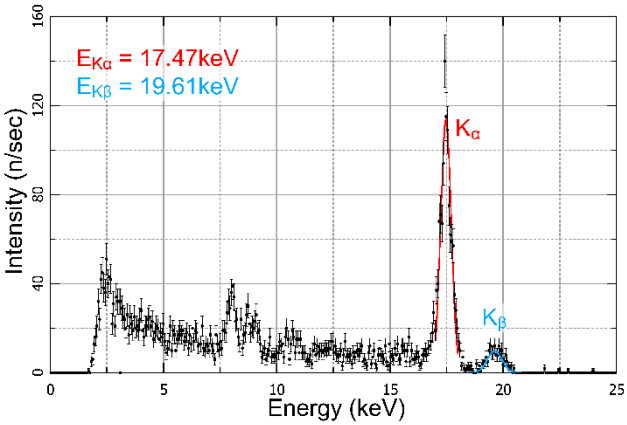

Figure C6: Characteristic X-Ray for Molybdenum (Mo)

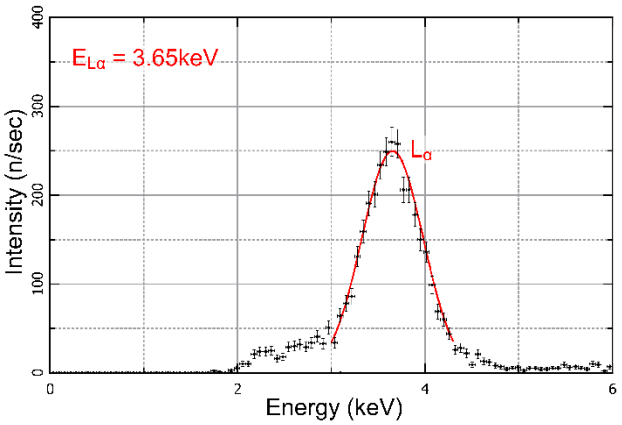

Figure C7: Characteristic X-Ray for Antimony (Sb)

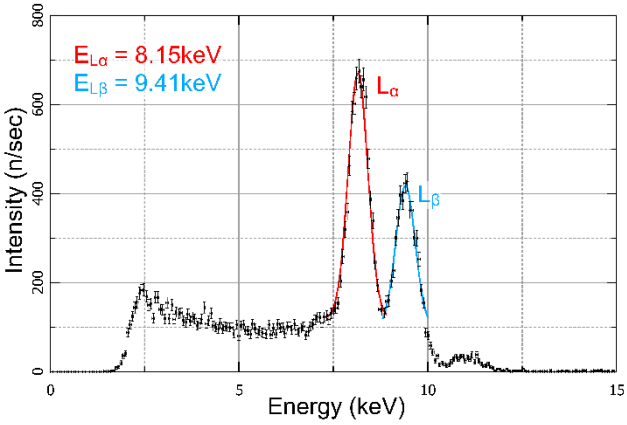

Figure C8: Characteristic X-Ray for Tantalum (Ta)

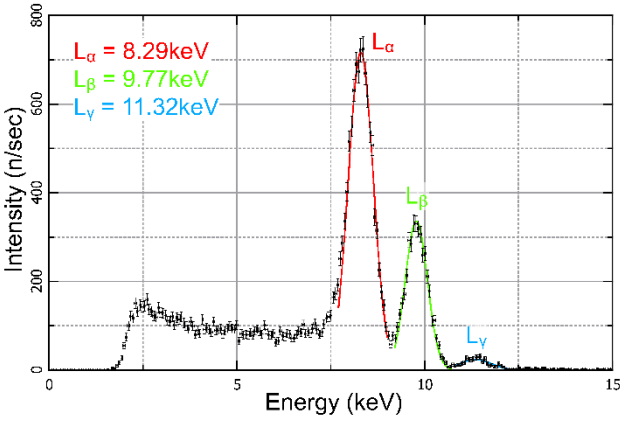

Figure C9: Characteristic X-Ray for Tungsten (W)

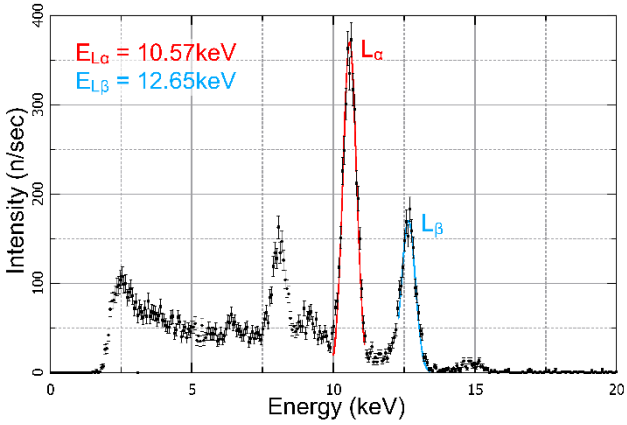

Figure C10: Characteristic X-Ray for Lead (Pb)

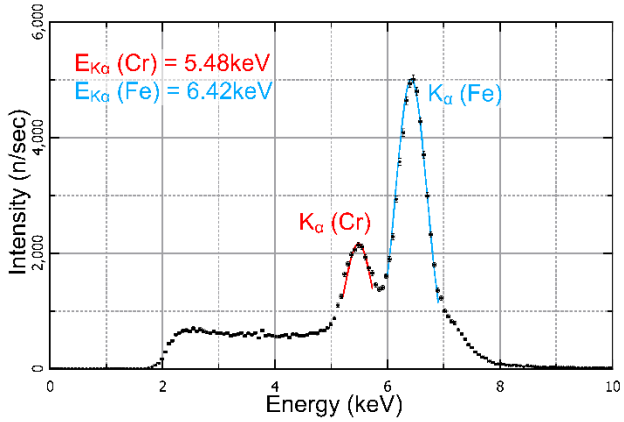

Figure C11: Characteristic X-Rays for Steel (Cr & Fe)

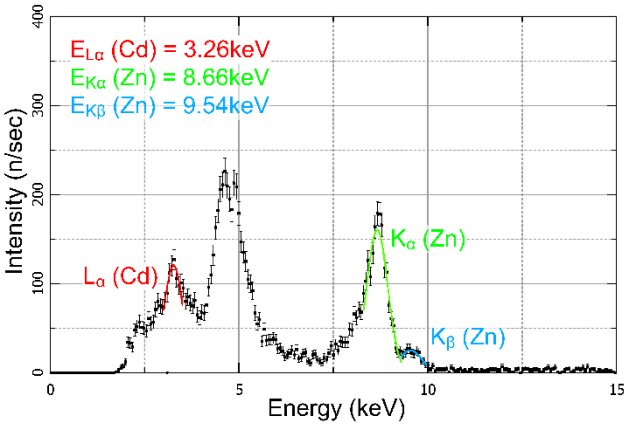

Figure C12: Characteristic X-Rays for Cadmium Paint (Cd & Zn)

Appendix D: Wavelength of Characteristic X-Rays for Copper

Starting with equation (C1) for minimum wavelength:

$$\lambda_{min} = \frac{c}{\nu} = \frac{ch}{eV} \quad \textbf{(D1)}$$

Calculating using energy centroids as seen in **Fig. C1**:

$$\lambda_{K\alpha 1} = \frac{(299792458 m/s)(4.1357\times10^{-15} eV\cdot s)}{8070 eV} = 1.54 \pm 0.057 \text{ Å} \quad \textbf{(D2)}$$

$$\lambda_{K\beta 1} = \frac{(299792458 m/s)(4.1357\times10^{-15} eV\cdot s)}{8900 eV} = 1.39 \pm 0.057 \text{ Å} \quad \textbf{(D3)}$$

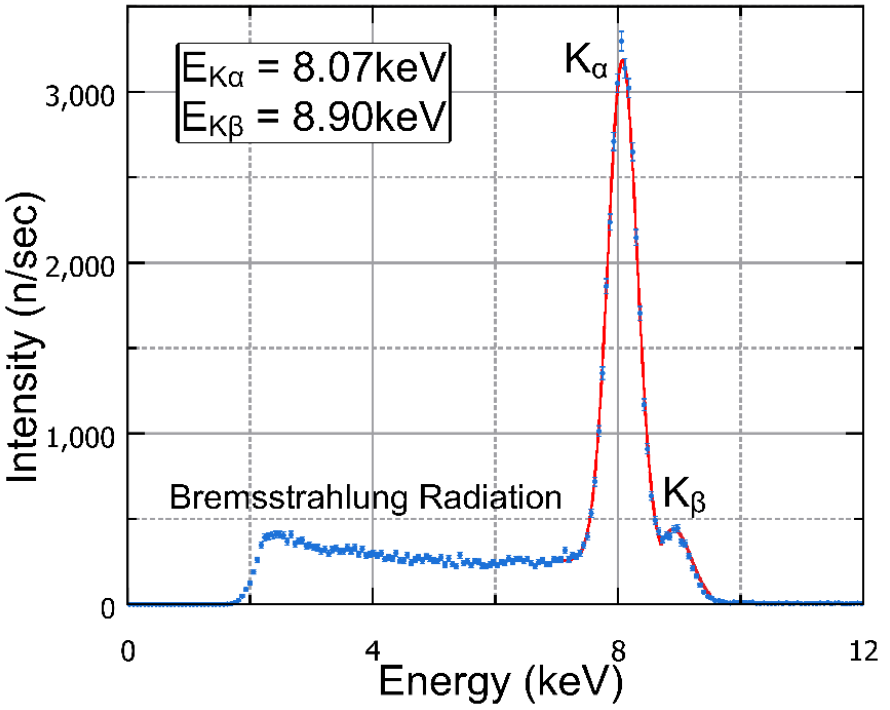

Figure D1: Characteristic X-Rays of Copper (Cu). *K-shell emissions of copper on a plot of x-ray intensity as a function of energy (keV). Bremsstrahlung radiation is characterized by continuous low intensity x-rays: can be seen from approximately 2 – 7keV. Two characteristic x-rays of copper are characterized by sharp peaks, with centroids $K_{\alpha 1}$ located at 8.07keV, and $K_{\beta 1}$ located at 8.90keV. Error in intensity is the square root of n, per the Poisson distribution, and error in energy ½ the bin quantization of energy as seen in Appx. B. To calculate the wavelength of the copper x-ray, equation (1) is utilized.*

Appendix E: Crystals Tested for Bragg's Law

Crystal	Order (n)	X-Ray Type	θ (±0.05°)	Exp. Lattice Spacing (Å)	Known Lattice Spacing (Å) [4]	Percent Error (%)	χ^2/dof
NaCl	1 1	$K_{\alpha 1}$ $K_{\beta 1}$	15.61 14.15	2.847±0.016 2.854±0.016	2.820	0.96 1.21	0.20
LiF	1 1	$K_{\alpha 1}$ $K_{\beta 1}$	22.38 20.08	2.027±0.023 2.017±0.023	2.014	0.65 0.15	0.24
KCl	1	$K_{\alpha 1}$	13.84	3.211±0.040	3.147	2.03	0.02
Unknown	1 1	$K_{\alpha 1}$ $K_{\beta 1}$	13.56 12.20	3.284±0.027 3.289±0.027	3.298	0.55 0.85	0.14

Table E1: Sample Crystals for Testing Bragg's Law. *Angle of diffraction θ is the centroid (μ) of a gaussian fit for a crystal's peak intensities. Exp. lattice spacing is calculated using equation (2) with the diffraction order, angle θ, and the calculated wavelength of copper as seen in Appx. D. Error in angle θ is due to lag in the carriage arm motor, and error in exp. lattice spacing is a propagation between error in angle and error in wavelength (from energy bin width).*

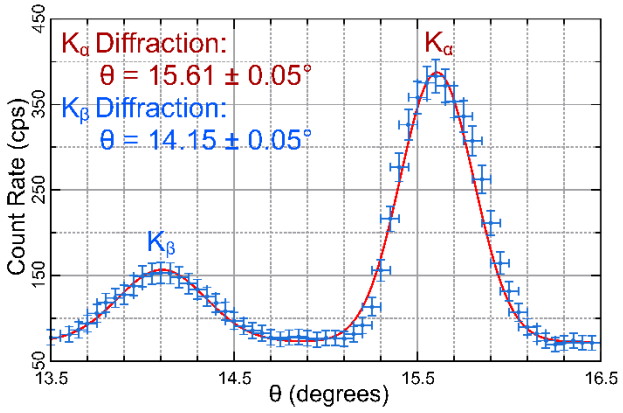

Figure E1: Bragg Diffraction Plot for NaCl

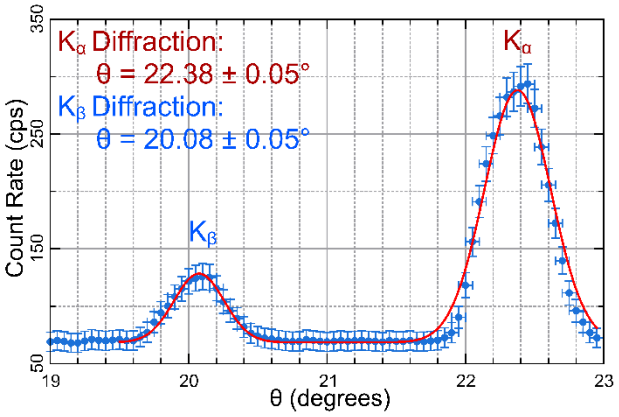

Figure E2: Bragg Diffraction Plot for LiF

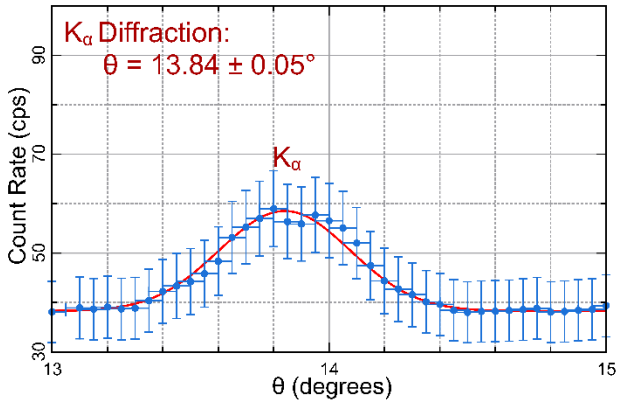

Figure E3: Bragg Diffraction Plot for KCl

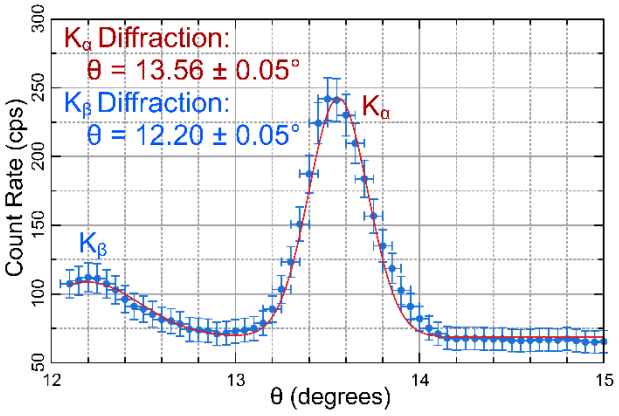

Figure E4: Bragg Diffraction Plot for Unknown Crystal

Supplementary Information (S.I.)

S.I. 1: X-Ray Tube

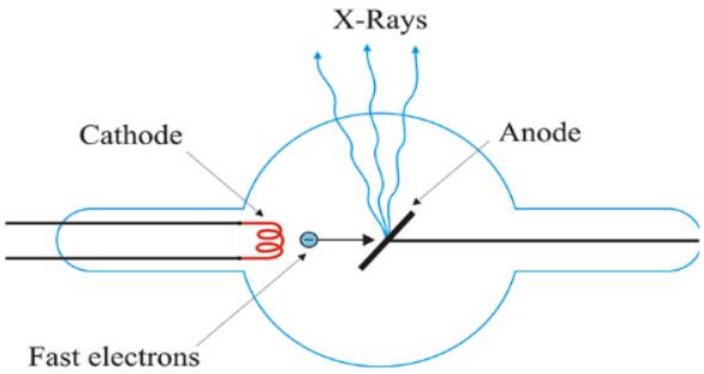

S.I. 1 Fig. 1: Diagram of an X-Ray Tube. *A beam of electrons is accelerated through high electrical potential between a heated cathode and a copper anode target. X-Rays are released.*

S.I. 2: Siegbahn X-Ray Notation

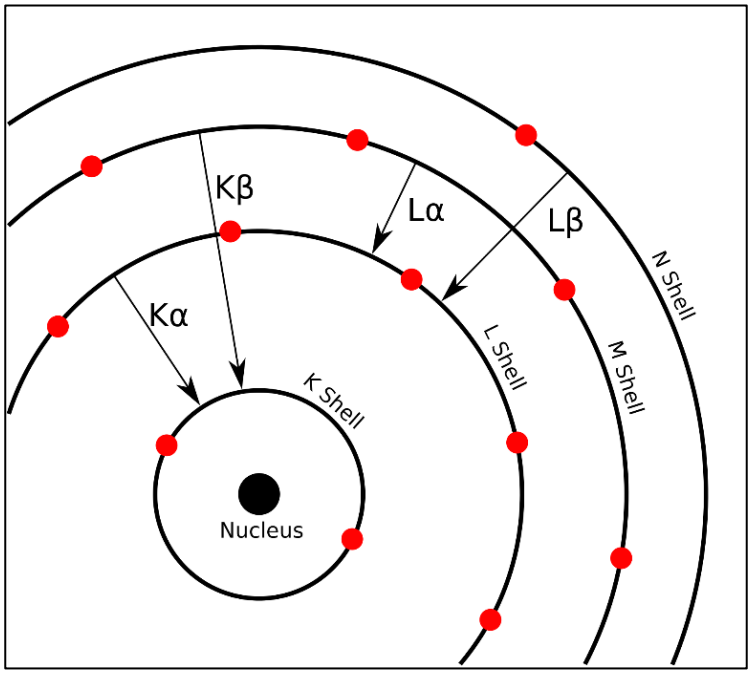

S.I. 2 Fig. 1: Characteristic X-Ray Notation as it relates to the Bohr Atomic Model: *Starting from the left, an electron which was ejected from the K-shell (principal quantum number n = 1) is replaced by an electron in the L-shell (n = 2) to fill its vacancy. The characteristic x-ray is therefore referred to as a K_α emission. On the far right, the L_β emission line is represents an electron which was ejected from the L-shell (n = 2) and replaced by an electron from the N-shell (n = 4): therefore, referred to as an $L\beta$ emission.*

Siegbahn notation will be used in this experiment for the sake of simplicity.

Using Bohr's atomic model, the letters K, L, M, and so-forth correspond to the orbital from which an electron is ejected once bombarded with radiation (K-shell: n = 1, L-shell: n = 2, M-shell: n = 3, etc.). The subscripts α, β, γ, and so-forth correspond to the orbital from which the electron filling the vacancy comes from relative to the vacant shell, (α: n + 1, β: n + 2, γ: n + 3, etc.). For this experiment, we will be focusing on K and L emission lines. Due to the higher energy emissions of M and N-shell emissions, our x-ray detector is unable to accurately detect them.